Electron magnetic moment from geonium spectra: Early experiments and background concepts

Robert S. Van Dyck, Jr., Paul B. Schwinberg, and Hans G. Dehmelt
Department of Physics, FM-15, University of Washington, Seattle, Washington 98195
(Received 21 May 1984; revised manuscript received 19 July 1985)

The magnetic moment of a free electron has been measured by observing both its low-energy spin and cyclotron resonances (at $\nu_s=\omega_s/2\pi$ and $\nu_c=\omega_c/2\pi$, respectively) by means of a sensitive frequency-shift technique. Using radiation and tuned-circuit damping of a single electron, isolated in a special anharmonicity-compensated Penning trap, also cooled to 4 K, the electron's motion is brought nearly to rest, thus preparing it in a cold quasipermanent state of the geonium "atom." The magnetic-coupling scheme, described as a continuous Stern-Gerlach effect, is made possible through a weak Lawrence magnetic bottle which causes the very narrow axial resonance, at $\nu_z=\omega_z/2\pi$ for the harmonically bound electron, to change in frequency by a small fixed amount δ per unit change in magnetic quantum number. Spin flips are indirectly induced by a scheme which weakly drives the axial motion at the $\nu_a=\omega_a/2\pi$ spin-cyclotron difference frequency within the inhomogeneous magnetic field, thus yielding a measure of $\omega_a\equiv\omega_s-\omega_c$. The magnetic moment μ_s in terms of the Bohr magneton μ_B equals $\frac{1}{2}$ the spin's g factor, which in turn is described by ω_s and ω_c: $g=2\mu_s/\mu_B=2\omega_s/\omega_c$. In a Penning trap, however, these resonance frequencies are obtained from the observed cyclotron frequency at $\omega_c'=\omega_c-\delta_e$ and the observed anomaly frequency at $\omega_a'=\omega_s-\omega_c'$, which are related by the small electric shift δ_e computed using the measured axial frequency and $2\delta_e\omega_c'=\omega_z^2$. This last expression, derived for a perfectly axially symmetric trap, happens to be practically invariant against small imperfections in the electric quadrupole field (error in $\omega_c<10^{-16}$). The magnetic-bottle-determined line shapes are analyzed and found to have sharp low-frequency edge features which correspond to the electron being temporarily at the trap center and at the bottom of the magnetic well. Relativistic shifts are considered and found to be $<10^{-11}$. Our result at the time of submission, $g/2=1.001\,159\,652\,200\ (40)$, is the most accurately determined parameter of any elementary charged particle which in addition can be directly compared with theory.

I. INTRODUCTION

The first *experiments* to measure the magnetic moment on free electrons were attempted by Dicke[1] at Princeton. The first successful work was that of Louisell, Pidd, and Crane[2] who reported data accurate to 1% for the magnetic moment of 420-keV electrons. The 1% accuracy achieved did not yet yield an experimental free-electron value for the anomalous part a of the g factor, $a=(g-2)/2\approx 0.001\,19$, previously measured on electrons bound in atoms. On free electrons the anomaly was first measured[3] to 3% at the University of Washington by Dehmelt. In this experiment, electrons stored in the field of a positive-ion cloud diffusing in a dense inert gas were polarized by spin-exchange collisions with an optically polarized sodium vapor and depolarized by magnetic resonance. By substituting a high-vacuum quadrupole trap for the space-charge field and an atomic beam for the alkali vapor, Dehmelt and Major developed the ion-storage-collision technique and demonstrated it in a magnetic resonance experiment on He^+ ions.[4] This ion-storage collision technique was then adapted to electrons in Mainz by Gräff, Major, Roeder, and Werth and by Gräff, Klempt, and Werth, who produced a measurement[4,5] of a. However, with an accuracy only 100 times better than the Seattle optical-pumping experiment, the Mainz group was never able to compete with the Michigan workers,[6] who earlier reported an error limit of only 2 parts in 10^5 in a.

All these experiments owed a debt to the founding fathers of magnetic resonance: Rabi, Bloch, and Purcell. Since these beginnings, a number of other workers have contributed much to the progress of the field as have proposals[7] put forth even earlier. Already in 1927 Brillouin proposed measurements on free electrons by a type of axial Stern-Gerlach effect. The spinning electron had been introduced by Goudsmit and Uhlenbeck only two years before. This had occurred over the initial objections[8] which Wolfgang Pauli had raised in defense of his concept of the "classically nondescribable two-valuedness of the quantum-theoretical properties" of the electron. Nevertheless, the final acceptance[9] of the term "spin" for the specifically atomic phenomenon in question must be considered as not entirely satisfactory. The term spin evokes the notion of a miniature golf ball rotating about an axis through its center of mass and clashes with Dirac's only slightly later concept of a point electron. This point electron executes a spontaneous periodic quasiorbital motion at the speed of light,[10] the *Zitterbewegung*[11] of Schrödinger, which moreover Huang showed[12] to be circular and to be accompanied by the (orbital) angular momentum of $\hbar/2$ and the magnetic moment of one Bohr magneton now conventionally attributed to "spin." The weakness of the spinning-golf-ball picture is also revealed by the vanishing of magnetic-moment-related interaction effects in close e^-/e^+ high-energy collisions. What remains is a soft quasiorbital structure of radius about one Compton wavelength/2π

formed by the circular *Zitterbewegung* of the hard point electron of dimensions $<10^{-16}$ cm. It is this structure, on which measurements of the intrinsic magnetism of the electron provide information. While the above constitutes a certain justification of Pauli's initial rejection of the spinning-electron model as "Neue Irrlehre," Pauli on the other hand overshot the mark when he attempted to prove that spin and magnetism of the free electron could not be measured[8,13] by a suitable variant[7] of the Stern-Gerlach experiment. In fact invention of the continuous Stern-Gerlach effect[14] for a trapped electron or positron by Dehmelt and Ekstrom has enabled the present researchers to measure the g factors for e^-/e^+ with error limits 2 and 4 orders of magnitude smaller, respectively, than the best previous work.[6]

The Zeeman effect has long been used in identifying unknown atomic spectra and energy eigenstates. Thus, the structure of an atomic state is reflected in its g factor, i.e., the ratio of the precession frequencies for the state under study, ω_p, to that of a suitable atomic reference state in the same field, ω_p^*. As this standard precession frequency ω_p^*, the natural choice was the Larmor precession associated with any purely orbital electron motion in an atom. Because of difficulties in the experimental realization of ω_p^*, Gardner and Purcell substituted $\omega_c/2$ for ω_p^* which it should equal under certain conditions, where ω_c is the electron cyclotron frequency. We wish to emphasize here that it is reasonable to define the g factor as the ratio of two observable frequencies. This is in keeping with our general philosophy of sticking closely to observables and to avoid emphasizing quantities such as mass, charge, and magnetic field, which, each by themselves, are less accurately known than the frequencies. The subject is more fully reviewed in Refs. 6 and 15. For any rigid classical gyromagnetic body whose charge is strictly tied to the mass and distributed in proportion to the mass density it should also hold, as for atomic states of purely orbital angular momentum,

$$g \equiv 2\omega_p/\omega_c = 1 \ , \tag{1.1}$$

where ω_p and ω_c now are the precession and cyclotron frequencies of the body. An empirical g factor $\neq 1$ would consequently imply a charge distribution not proportional to the mass density in a classical gyromagnetic body, or any nonclassical body. In accordance with the above, we may define the g factor of the free electron as

$$g \equiv 2\omega_s/\omega_c \tag{1.2}$$

in the limit of low kinetic energy and magnetic field B_0. Here ω_s is the spin precession frequency. Also, as $\omega_s = (\mu_s/\frac{1}{2}\hbar)B_0$ and $\omega_c = (e/m_0c)B_0$ hold,

$$\mu_s = (\omega_s/\omega_c)\mu_B \tag{1.3}$$

follows for the magnetic moment in Bohr magnetons, $\mu_B \equiv (e\hbar/2m_0c)$.

Previous to our work, the most precise g-factor data came from the Michigan group:[6]

$$\tfrac{1}{2}g(e^-) = 1.001\,159\,656\,700\ (3500) \ . \tag{1.4}$$

That experiment was done on bunches of $\approx 10^4$ energetic (100 keV) electrons localized to about 20 cm for ≈ 6 ms in a completely magnetic Lawrence trap formed by a slightly inhomogeneous 0.1-T field. The electron spins were polarized and analyzed by Mott scattering. These workers measured the spin-cyclotron-beat frequency $\omega_s - \omega_c$ directly by a free-precession technique. However, for the appropriate ω_c data, they had to rely on other experiments performed in other laboratories. By contrast, the Washington experiment is carried out on the same individual cold (≈ 1 meV) electron quasipermanently confined to $<100\ \mu$m in a Penning trap (electric quadrupole field plus homgeneous 2—5 T magnetic field) where both $\omega_s - \omega_c$ and ω_c are measured on the same electron by rf resonance techniques. The spin direction is analyzed by the continuous Stern-Gerlach effect mentioned already. In these experiments we collected data at 1.9, 3.2, and 5.1 T in 40 runs, and were able to quote

$$\tfrac{1}{2}g(e^-) = \omega_s/\omega_c = 1.001\,159\,652\,200\ (40) \ . \tag{1.5}$$

For this result, the frequencies ν_s, ν_c ranged from 51—143 GHz, ν_a ranged from 60—166 MHz, and $\delta_e/2\pi$ ranged from 35—10 kHz, with ν_z constant at 60 MHz. To reach the accuracy quoted in (1.5), it was necessary to employ an approximate analysis of the line shape as explained in Sec. VI. This experimental result approximately agrees (within the combined error limits of experiment and calculations) with the present best theoretical g value

$$\tfrac{1}{2}g(e^-) = 1.001\,159\,652\,459\ (135) \tag{1.6}$$

calculated on the basis of QED from the experimental Josephson-effect value for the fine-structure constant. The status of these calculations is reviewed by Kinoshita and Sapirstein.[16]

In another development, a proposal to continuously trap via radiation damping small numbers of positrons from a weak β^+ source, sealed into the electron tube, has been realized by Paul Schwinberg in his doctoral thesis. This has enabled us to study the positron in exactly the same fashion as the electron, realizing essentially the same error limits in the g factor. Our precision measurements of the $e^\pm$ g factors, which reached the 50 parts in a trillion error level, provide the most stringent confirmations of quantum electrodynamic theoretical calculations to date. The identity of the g values found to this accuracy is consistent with the mirror symmetry of this *charged* particle—antiparticle pair demanded by the *CPT* theorem to the same accuracy, independent of experimental input data determined elsewhere. The accuracy is only exceeded in high-energy experiments of another nature on the *neutral* $K,\bar{K}$ particle-antiparticle pair.[17] General reviews of g factors of leptons have been published by Tolhoek,[1] Farago,[18] Crane,[6] Rich,[6] and by Field, Picasso, and Combley.[15] Klempt[19] and Dehmelt[20] have discussed progress in low-energy free-electron work. Stored-ion-spectroscopy experiments have been reviewed by Dehmelt,[4] Schuessler,[21] Werth,[22] Wineland,[23] and Wineland, Itano, and Van Dyck.[24] The development of high-resolution monoparticle spectroscopy techniques at the University of Washington[25] has also been described by Dehmelt. Our individual stored-electron (geonium) experiments on the g

factor[26] have been reported more briefly before. Various theoretical developments have been discussed by Lepage[27] and by Kinoshita and Lindquist.[28]

The purpose of this paper is to describe in greater detail the most salient features of our early geonium experiments and to give some necessary background. In Sec. II the basic concepts of the experiment are discussed with attention to the axial harmonic oscillation and the frequency-shift detection mechanism. Some early results showing actual observations of spin flips are given as well. In Sec. III the classical orbits of the cyclotron and magnetron motion are explored along with a discussion of the symmetry of the trapping fields. Section IV deals with the quantum mechanics of geonium. Transition frequencies are investigated in this section in order to arrive at the relativistic couplings between the various motions and particular attention is given to the anomaly resonance and its observable transition rate. Section V highlights the magnetic bottle as producing a "continuous" Stern-Gerlach effect for separating the magnetic quantum states. In Sec. VI some general characteristics of the line shapes associated with these magnetic resonances are discussed. Section VII is a brief summary of this paper.

It is also the intention of the authors to develop a sequel to this paper in the near future with the following emphasis: Section I will discuss the actual electron tube with particular attention to the refinement in anharmonicity compensation, as well as the reliable all-metal vacuum envelope. Section II will expand on the detection of the axial resonance (as introduced briefly in Sec. II of the present paper) and describe the isolation of a single charge. Section III will explain how the metastable magnetron motion is cooled and discuss various methods of measuring its frequency and radius. Section IV will deal with the production of cyclotron resonances and will exhibit improvements in excitation and resolution of the low-frequency edge. Section V will discuss the production of the anomaly resonances and will highlight the exact line-shape fitting according to a Brownian motion line-shape theory. Finally in Sec. VI results of this work on electrons will be summarized up to the present with a comparison with theory. Also a discussion of the physical limitations for future improvements will be given. It is further planned that a separate paper will be written in order to address the particular application of this geonium experiment to a single positron and to compare corresponding g factors and masses with the electron.

II. CONCEPT OF THE EXPERIMENT

In the early part of the last decade, it became clear that the best way to reach the goal of making ultrahigh-precision measurements of the free-electron g factor was to reduce the number of trapped electrons to its smallest possible quantity, namely one. It was at this juncture that much of our efforts were redirected toward developing many of the techniques now used routinely by the various mono-ion spectroscopy groups at the University of Washington. Initially, our efforts were concentrated on generating a scheme that would allow the continuous observation of a single electron. The solution was to drive the axial motion of the trapped charge like a simple anharmonic oscillator and to use appropriately phased synchronous detection methods since it is well known that narrow-band mixing schemes have intrinsically a greater signal-to-noise ratio than the previous wide-band noise-detection methods useful in ion-cloud work.[29] The ultimate success of this early effort culminated in the first ever detection of the axial motion of a *single* electron trapped in a Penning trap[30] which we subsequently referred to as the "monoelectron oscillator" (see Fig. 1). At this point, it is prudent to outline the basic features of the Penning trap which is used as an electromagnetic cage to trap the electron and then describe the developments in technique which eventually led to the most precise measurement *ever* of the free electron's spin g factor.

A. Schematic of experiment

After the early work using a standard electromagnet (≈ 0.8 T) and liquid-nitrogen cooling, it was decided that the chances for success were greater if we increased the magnetic field by about an order of magnitude and likewise reduced the temperature of the trapping environment to 4 K. As shown in Fig. 2, a superconducting solenoid, capable of achieving ≈ 6 T was obtained and the Penning trap, consisting essentially of two end caps and a ring electrode (also shown in more detail in Fig. 1), was immersed in a liquid-helium bath. In order to take advantage of the quiet environment, the LC circuit, tuned to the electron's driven axial motion, was also placed in the 4-K bath, as close to the trap as possible along with the appropriate preamplifier. The electron's Brownian (thermal) axial motion along the axis of symmetry (at $\nu_z \approx 60$ MHz) is quickly reduced to a minimum via its coupling to this tuned circuit. Its cyclotron motion, at $\nu_c \approx 51$ GHz in a $B_0 = 1.8$ T axial magnetic field, also quickly thermalizes to 4 K by radiation damping and only the lowest Rabi-Landau levels with associated microscopic orbits are ap-

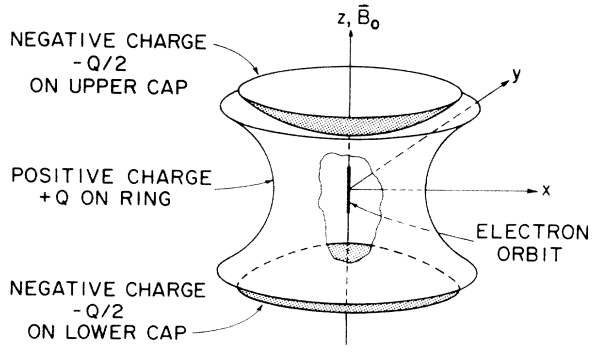

FIG. 1. *Monoelectron oscillator* mode of electron in Penning trap, the geonium "atom." The electron moves only parallel to the magnetic field $\mathbf{B}_0$ and along the symmetric axis of the electrode structure. Each time it gets too close to one of the negatively charged caps, it is turned around and an oscillatory motion results.

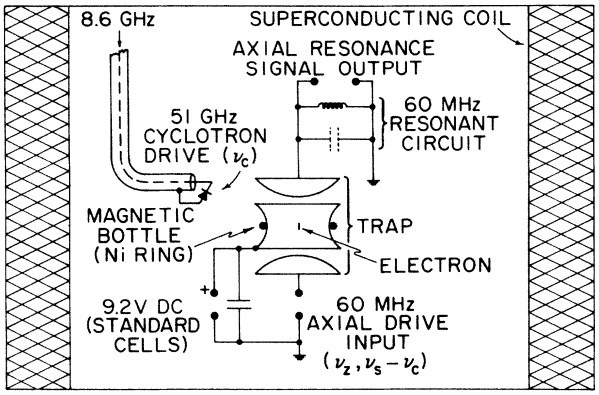

FIG. 2. Geonium spectroscopy experiment (schematic). This apparatus allows the measurement of the cyclotron frequency, ν_c, and the spin-cyclotron-beat (or anomaly) frequency, $\nu_a \equiv \nu_s - \nu_c$, on a single electron stored in a Penning trap at ≈ 4 K ambient. Detection is via Rabi-Landau level-dependent shifts in the continuously monitored axial resonance at frequency ν_z, induced by a weak magnetic bottle.

preciably occupied. The diameter of the metastable magnetron (drift) motion at $\nu_m \approx 35$ kHz is minimized by a specially developed sideband cooling technique, which resembles optical pumping. Also visible in Fig. 2 is the nickel ring located in the midplane of the main-ring electrode which produces the weak magnetic bottle, whose function is described in more detail in Sec. II C.

B. Axial harmonic oscillation

An approximate form for the potential near trap center in a device which has even-order reflection and rotational symmetry such as the Penning trap is given in cylindrical coordinates r,z (through fourth order) by

$$\frac{\phi(r,z)}{U_0} = \frac{r^2-2z^2}{4Z_0^2} + C_4 \frac{8z^4-24r^2z^2+3r^4}{16Z_0^4} , \tag{2.1}$$

where U_0 is the applied ring-to-end-cap potential, $2Z_0$ is the minimum end-cap separation, and C_4 is a coefficient that depends on the geometry of the actual trap. In order to enhance the first term which is proportional to the second-order Legendre polynomial P_2, the electrodes are machined (to tolerances of 0.0015 cm) as hyperbolas and placed along the equipotentials associated with P_2 (see Fig. 3). Since the axial dependence defines a harmonic-oscillation potential (when U_0 is chosen with the proper sign), the frequency of this axial motion is determined by the electric spring constant k_e associated with the linear restoring force obtained from the gradient of the potential

$$F_e^z = -k_e z = e\frac{\partial\phi(r,z)}{\partial z} , \tag{2.2}$$

where $-e$ is the electron's charge. For a harmonic oscillator, $k_e = m\omega_z^2$, and using only the first term in (2.1), it follows that the axial oscillation frequency is given by

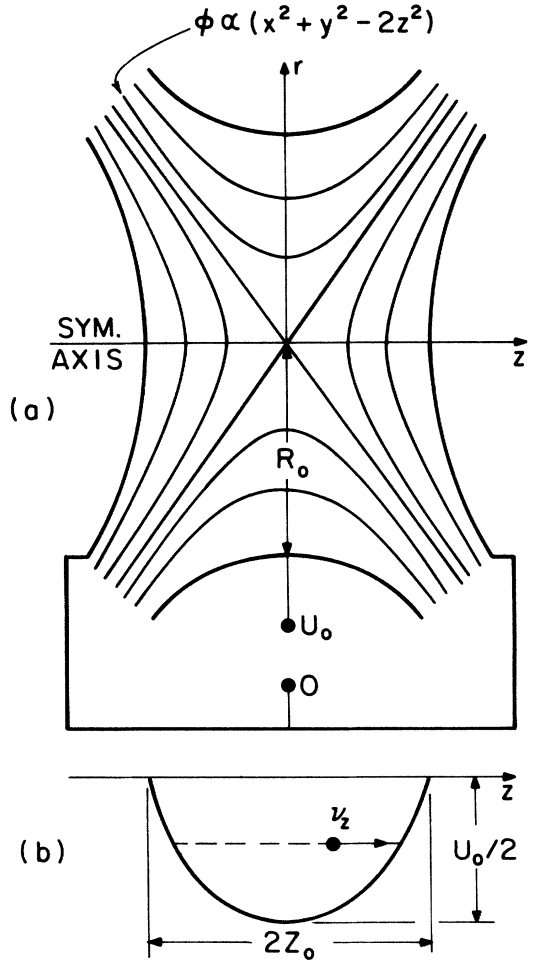

FIG. 3. Hyperbolic electrode configuration employed in the Penning trap. Application of dc voltage U_0 to the ring, relative to the end caps, creates an axial well of depth $eU_0/2$ for the choice $R_0^2 = 2Z_0^2$.

$$\omega_z^2 = \frac{eU_0}{mZ_0^2} . \tag{2.3}$$

In order to measure this frequency, a drive signal is applied to the end cap opposite to the one attached to the detection tuned circuit and the image current induced by the electron's motion in the LC circuit is observed. However, early in the course of the experiment, it became clear that one could not drive directly at the same frequency to which the LC circuit is tuned, since the strong drive signal would swamp the extremely weak, driven axial motion signal ($\lesssim 10^{-13}$ A). Thus, a sideband scheme was incorporated whereupon a 1-MHz drive is added to the 9.2-V dc ring potential, shown in Fig. 2, in order to modulate the well potential and create sidebands at $\nu_z \pm 1$ MHz upon the axial motion. By driving one of these sidebands and detecting the resulting motion on resonance (at ν_z), the feed-through problem was greatly reduced.

Now older 3-electrode Penning traps consisting of only two end caps and a ring electrode as shown in Fig. 1, could resolve the axial resonance defined by Eq. (2.3) only to 1 part in 10^5, primarly due to the anharmonic contribu-

tions obtained from the second term in Eq. (2.1) (which is proportional to the fourth-order Legendre polynomial). Thus, a major modification was attempted at this point and two guard rings were included (placed between each end cap and ring electrode) which allowed the net anharmonicity to be nulled out[14,31] by applying an additional compensation potential to the guards. The result was the typical axial resonance shown in Fig. 4, in which the linewidth was reduced a hundredfold, allowing a frequency resolution that approached 1 part in 10^8.

C. Frequency-shift detector

These well-resolved axial resonances now form the basis of the apparatus as a frequency-shift detector. By adjusting the phase of the drive signal we obtain the dispersion-type response shown in Fig. 4, which is then used as an error signal to be integrated and fed back to the ring electrode in order to keep the axial resonance locked to a very precise and stable frequency synthesizer. The integrated "correction" voltage now represents our frequency-shift signal which may be continuously monitored in order to record any changes in the very precise and stable axial resonance frequency.

However, we are primarily interested in magnetic transitions whose basic frequencies are in excess of 50 GHz. Since these frequencies are too high to easily observe directly, a technique was proposed[14] that uses a weak magnetic bottle to generate the required magnetic coupling into the exclusively electrical axial resonance. The complete description of this bottle field is discussed in Sec. V, but for present purposes, it suffices to note that along the axis of symmetry, the magnetic field increases quadratically such that

$$B_z = B_0 + \beta z^2 , \tag{2.4}$$

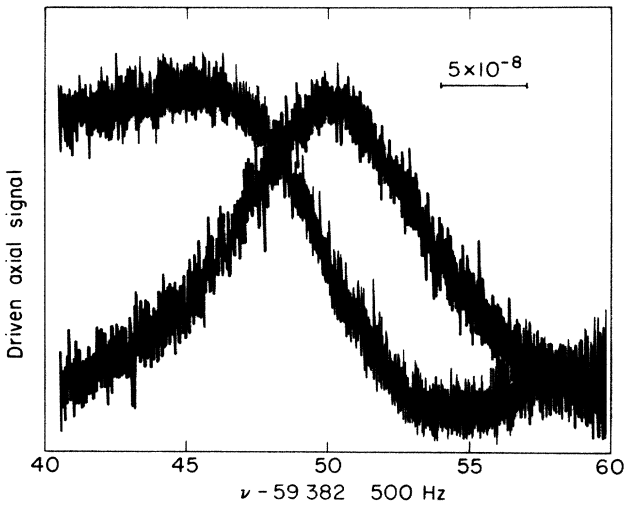

FIG. 4. Axial resonance signals at ≈ 60 MHz. The signal-to-noise ratio of this ≈ 8 Hz wide line corresponds to a frequency resolution of 1 part in 10^8. Both absorption and dispersion modes are shown with the latter mode appropriate for the frequency shift detection scheme employed in these geonium experiments.

where β defines the strength of this bottle and $\beta z^2 \ll B_0$. Since the magnetic moment has a pseudopotential energy in the strong axial magnetic field, $U_m = -\boldsymbol{\mu}\cdot\mathbf{B}$, it follows that a small additional axial binding energy (for negative μ_z)

$$U'_m = -\mu_z \beta z^2 \tag{2.5}$$

appears where μ_z is now the z component of $\boldsymbol{\mu}$. The corresponding additional restoring force is given by

$$F_m^z = -\frac{\partial U'_m}{\partial z} = 2\mu_z \beta z \tag{2.6}$$

which must be added to the electric force in order to arrive at the following expression:

$$m_0 \omega_z^2 = m_0 \omega_{z0}^2 - 2\beta\mu_z \, . \tag{2.7}$$

Since the last term is a magnetic interaction, it is small and the last equation simplifies to

$$\omega_z = \omega_{z0} - \beta\mu_z / m_0 \omega_{z0} \tag{2.8}$$

which now illustrates that observing small frequency shifts $\delta\nu_z$ in the electric axial frequency will yield information on the state of the *axial* component of the magnetic moment. This description then forms the basis of the continuous axial Stern-Gerlach effect which is described more fully in Sec. V.

D. Early results—observing spin flips

In this scheme, the first applied axial magnetic bottle caused the axial frequencies ν_z associated with the two spin states $m = \pm\frac{1}{2}$ to differ by ≈ 2.5 Hz. Historically, the first spin flip documented by this technique is shown in Fig. 5. The figure also shows very clearly why it was absolutely necessary to lower the ambient temperature to ≤ 4 K: The scheme detects the thermal random variations in the cyclotron level n due to the associated changes in the effective magnetic moment just as well as a spin flip.

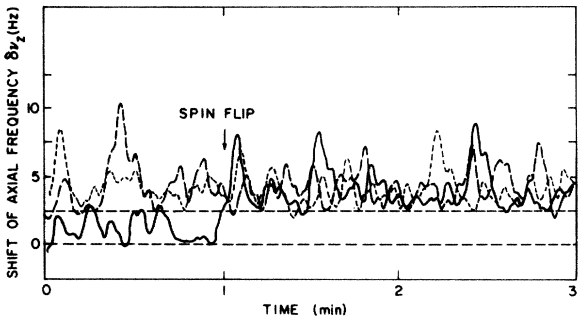

FIG. 5. First recorded spin flip seen in the monoelectron oscillator (geonium). Because of the random fluctuations in the thermally excited cyclotron motion, the axial frequency shift $\delta\nu_z$, associated with an earlier magnetic bottle, shows a corresponding unsymmetric fluctuation which always stays above a fixed floor for a given spin direction. This floor, however, suddenly changes by 2.5 Hz when the spin is flipped, which occurs occasionally near the axial resonance, $\nu_z - \nu_a \approx 2$ kHz. No auxiliary ν_a drive was used. Three superimposed traces are seen, and only the heavy one shows the spin flip.

Even at 4 K in fact, the asymmetric cyclotron energy fluctuations (if one would not follow them fast enough) tend to mask the spin flip. Nevertheless, by focusing on the floor of the fluctuations corresponding to the level $n=0$, which the electron preferentially occupies, one may recognize the spin flip.

While the ultimate goal of the experiment is a precise measurement of the ratio ω_s/ω_c with ω_s denoting the spin resonance frequency, it would not be advisable to attempt to induce spin flips (which we now know how to detect) by irradiating the electron with a magnetic microwave field at ω_s. The main reason for this is that ω_s/ω_c may conveniently be obtained in the form

$$\omega_s/\omega_c \equiv [(\omega_s-\omega_c)/\omega_c]+1 , \tag{2.9}$$

where, as in the Michigan experiments,[6] $\omega_s-\omega_c \equiv \omega_a \approx 10^{-3}\omega_c$ may be measured directly with a relative precision comparable to that available for ω_s and ω_c. The ω_a measurement is greatly facilitated by using another aspect of the magnetic bottle. Merely by exciting an auxiliary forced axial oscillation through the bottle field at ω_a with an amplitude much smaller than the thermal motion at ω_z, a viable microwave magnetic field at $\omega_s=\omega_c+\omega_a$ may be produced as a combination "tone"[4(c)] with the free thermal cyclotron motion at ω_c.

The anomaly resonance produced in this fashion is shown in Fig. 6. The large width is attributed to a modulation of the B field by the random-amplitude thermal axial motion in the magnetic bottle, and may be qualitatively understood as follows. The noise electric field from the tuned circuit at the trap excites a (Brownian) ω_z motion of the complex amplitude $z_B e^{i\phi}$ while the resonant detection drive produces an excitation amplitude z_d. The total complex amplitude

$$\tilde{z}=(z_d+z_B e^{i\phi})e^{i\omega_z t} \tag{2.10}$$

then fluctuates in its magnitude $|\tilde{z}|$ with a time constant similar to the characteristic axial damping time of the electron ($\tau_z \approx 20$ ms):

$$|\tilde{z}|^2 = z_d^2 + 2z_d z_B \cos\phi + z_B^2 , \tag{2.11}$$

where the random phase ϕ and (real) amplitude z_B fluctuate with characteristic time $2\tau_z$. (Here $\tilde{z}$ is the complex coordinate with $\mathrm{Re}\{\tilde{z}\}=z$.) As an example, let $z_d^2=25\langle z_B^2\rangle_{\mathrm{av}}$ and approximate z_B^2 by $\langle z_B^2\rangle_{\mathrm{av}}$; then one sees that $|\tilde{z}|^2$ fluctuates approximately between the values

$$|\tilde{z}|^2 = \tfrac{26}{25}z_d^2 \pm \tfrac{2}{5}z_d^2 . \tag{2.12}$$

The magnetic bottle field increases $\propto z^2$, and therefore the bottle field, averaged over the ω_z motion, is proportional to $|\tilde{z}|^2$. Now our example shows that the average bottle field seen by the driven electron fluctuates over a range proportional to $\frac{4}{5}z_d^2=20\langle z_B^2\rangle_{\mathrm{av}}$, while purely thermal excitation would only yield a fluctuation range $\propto\langle z_B^2\rangle_{\mathrm{av}}$. As the spin relaxation time is practically infinite, this has important implications for how to reduce the unnecessarily large width of the anomaly resonance: turn off the detection drive while inducing the transition and look later for shifts in the axial frequency that indicate spin flips. Cyclotron and magnetron frequencies are measured by resonant excitation at ω_c and ω_m and likewise detected by the continuous Stern-Gerlach effect. The ω_m data then provide an important check of the electric-field symmetry assumed in the analysis of the data.

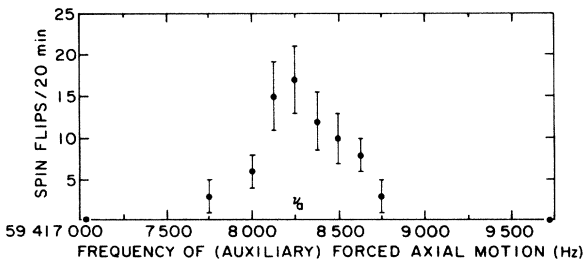

FIG. 6. Resonance at the spin-cyclotron-beat frequency ν_a in geonium. The auxiliary axial ν_a-drive amplitude has been adjusted such, that spin flips occur no faster than 1 min^{-1}, and can be conveniently counted in 20-min periods, during which the auxiliary drive frequency is kept constant.

III. CLASSICAL ORBITS

The main principle of the Penning trap is the following. The simplest motion of an electron in a homogeneous magnetic field B_0 is a trajectory along a field line parallel, say, to the z axis, with constant velocity. If a weak electric quadrupole field axially symmetric around the z axis of appropriate polarity is superimposed, the motion is still along a straight line but, because of the parabolic electric potential well of depth D_z now present, it is sinusoidally oscillatory at frequency ω_z, as described in Sec. II. The motion in the xy plane is easily analyzed for the special case of circular orbits (radius r) centered on the trap center (the origin). Because of the validity of Laplace's equation, the radial electric force F_e^r must have the form $F_e^r=m_0(\omega_z^2/2)r$, with m_0 the electron mass. The force F_e^r opposes the centripetal magnetic force $e(v/c)B_0$ with v the orbital velocity. Newton's second law then takes the form for circular orbits,

$$e(v/c)B_0 - m_0(\omega_z^2/2)r = m_0 v^2/r . \tag{3.1}$$

by introducing the circular frequency $\omega \equiv v/r$ and the cyclotron frequency

$$\omega_c \equiv eB_0/m_0 c \gg \omega_z , \tag{3.2}$$

it follows[4(a)] that

$$2\omega(\omega_c-\omega)=\omega_z^2 . \tag{3.3}$$

First we are primarily interested in the electric-field shift

$$\delta_e \equiv \omega_c - \omega_c' \tag{3.4}$$

which slightly changes the observed cyclotron frequency from ω_c to ω_c'. It should also be noted that the same electric field shift moves the observed anomaly frequency from ω_a to ω_a'. We obtain the desired expression for δ_e in terms of the measured frequencies ω_z and ω_c' merely by identifying ω with ω_c' and rewriting Eq. (3.3) as

$$\delta_e = \omega_z^2/2\omega_c' \ . \tag{3.5}$$

Next we see by substitution that $\omega = \omega_c - \omega_c'$ is the other root of the quadratic equation (3.3) for the frequency of circular motions possible in the trap. This is the frequency of the slow drift or "magnetron" motion at ω_m. However, the identity

$$\omega_m = \delta_e \tag{3.6}$$

is purely a property of a perfect trap. It is destroyed by any slight asymmetry or misalignment of the electric field.

The most general orbit may be obtained by superposing all three previously described simple orbits, two of which are shown in Fig. 7. The most amazing feature of the perfect Penning trap is that all three frequencies ω_c', ω_z, ω_m are constants of the trap; i.e., they do not depend on the location of the ion or electron in the trap. For a single electron with the parameter values $\nu_c' \approx 51$ GHz, $\nu_z \approx 60$ MHz, $\nu_m \approx 35$ kHz and for the thermal (or Brownian motion) excitation of cyclotron and axial motions at 4 K (i.e., the temperature of liquid helium), the general orbit consists of a very fast cyclotron motion of $2r_c \approx 600$ Å diameter around a slower moving guiding center. This guiding center in turn executes a fast axial oscillation of less than 0.1-mm peak-to-peak amplitude and a very slow metastable circular motion around the origin. It has so far not been possible to reduce its radius r_m below about 15 μm. The general equations of motion may be written

$$\begin{aligned} &\ddot{x} - \omega_z^2 x/2 + \omega_c \dot{y} = 0 \ , \\ &\ddot{y} - \omega_z^2 y/2 - \omega_c \dot{x} = 0 \ , \\ &\ddot{z} + \omega_z^2 z/2 = 0 \ . \end{aligned} \tag{3.7}$$

Their linearity justifies the superposition of simple orbits. One way to solve them is to use the complex notation $\zeta = x + iy$ which then yields

$$\ddot{\zeta} - i\omega_c \dot{\zeta} - \omega_z^2 \zeta/2 = 0 \ . \tag{3.8}$$

Setting $\zeta = e^{i\omega t}$ gives again Eq. (3.3) and the general solution

$$\zeta = r_c e^{i\omega_c' t} + r_m e^{i\omega_m t} \ , \tag{3.9}$$

where a complex phase factor for r_m has been suppressed by adjusting the origin of the time scale appropriately.

As practical traps will always show a small misalignment between electric and magnetic axes as well as small deformations of the symmetric electric field gradient, it is important to test the trap symmetry experimentally. Fortunately, relation (3.5) is practically invariant to such imperfections while ω_m is not. Thus the difference

$$\omega_m - \omega_z^2/2\omega_c' \simeq \omega_m - \delta_e \ , \tag{3.10}$$

expressible in measurable electron frequencies only, becomes a sensitive indicator of trap imperfections, which might require higher-order corrections to Eq. (3.5) for the frequency shift δ_e. One reason that we might expect any corrections to Eq. (3.5) to be of higher order is that the radial electron motion is dominated by the interaction with the large magnetic field along the z axis. Whatever distortions of the simple axially symmetric electric quadrupole potential the trap imperfections produce, the saddle point will remain very close to the geometrical center of the trap. Near the saddle point, the potential will be dominated by the quadrupole term, which in general will only be approximately axially symmetric. Also, the approximate symmetry axis will make a small angle with the direction of the magnetic field which coincides with the z axis. According to mathematical techniques commonly used in astronomy, an excellent approximation of the problem may be obtained by averaging the potential around the z axis before solving the problem. Stated in other words, the fast cyclotron rotation around and the fast axial oscillation along a magnetic field line average out the effects of *any* small unsymmetric part of the electric field on the electron orbit such that the above analysis of the perfectly symmetric trap retains its validity for ω_c' to first order. As can be seen,[32] the averaged axially symmetric field gradient, valid for cyclotron and axial motion only, has the principal axes x,y,z. Its components, $\bar{\phi}_{xx}, \bar{\phi}_{yy}, \bar{\phi}_{zz}$, are obviously related by

$$\bar{\phi}_{xx} = \bar{\phi}_{yy} = -\bar{\phi}_{zz}/2 \ , \tag{3.11}$$

where, for instance, $\bar{\phi}_{zz}$ equals the second derivative, taken along the z axis, of the unaveraged total electric potential ϕ, whose principal axes may differ from x,y,z in general.

By contrast the slow magnetron or drift motion is incapable of averaging the general field gradient. Instead, the magnetron motion becomes distorted following a noncircular orbit, along which ϕ_z vanishes and which departs from the xy plane. This explains why Eq. (3.6) loses its exact validity and $\omega_m - \delta_e$ now functions as an indicator of electric-field imperfections. The expected averaging of the general field gradient is confirmed[32] in classical and quantum-mechanical first-order perturbation calculations of ω_c'. The recent beautiful result of an exact solution[33] of the equations of motion for a general misaligned, distorted electric-field gradient,

$$\omega_c'^2 + \omega_z^2 + \omega_m^2 = \omega_c^2 \ , \tag{3.12}$$

may be expanded to yield

$$(\text{correction to } \delta_e) \approx (\omega_m/\omega_c')(\omega_m - \delta_e) \ . \tag{3.13}$$

In our experiments, this correction corresponds to $< 2\pi \times 10^{-5}$ Hz, a negligible value.

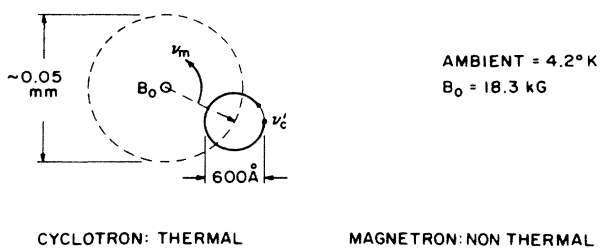

FIG. 7. Geonium orbits under thermal excitation at ≈ 4 K, showing xy motion only.

IV. QUANTUM MECHANICS OF GEONIUM

In geonium, quantum effects are important in the continuous Stern-Gerlach effect and in the calculation of transition probabilities. Even relativistic quantum mechanics is required to describe the relativistic couplings between the various resonances, and the fine structure[26(d)] of the cyclotron resonance itself. An experimental resolution as high as 1 part in 10^{11}, which is amply sufficient for resolution of the splittings, is conceivable, and the observation of this fine structure may become a superior alternative for the monitoring of the spin state.

In order to keep mathematical complexity at a minimum, we adapt various results given in the literature to our needs. Thus, good approximate energy eigenvalues for relativistic geonium may be obtained, simply by supplementing the published Schrödinger values with correction terms evaluated from a published exact closed solution of the zero-electric-field Dirac equation augmented by an anomalous moment term. In order to make the discussion of the energy eigenvalues more manageable, we introduce atomic units for Secs. IV A—IV D, but return to cgs units in Sec. IV E to more clearly reflect dimensions.

A. Schrödinger equation

The Schrödinger equation may be written ($c=\hbar=1$)

$$\left[\frac{\pi^2}{2m_0}+U+\frac{\omega_c\sigma_z}{2}\right]\psi=W_S\psi\ , \tag{4.1}$$

with

$$\pi=\mathbf{p}+e\mathbf{A}\ , \tag{4.2}$$

where ω_c is the zero-velocity cyclotron frequency defined in Eq. (3.2); m_0 and $-e$ are rest mass and charge of the electron, and U is the electrostatic potential energy associated with the charge in a Penning trap having axial frequency ω_z [see Eq. (2.3)]. Here, π denotes the kinetic momentum, $\mathbf{p}=-i\nabla$ the canonical momentum, $\mathbf{A}$ the vector potential associated with the magnetic field $\mathbf{B}_0=B_0\hat{\mathbf{z}}$, and σ_z is the axial spin operator. Sokolov and Pavlenko solved the problem[34] in 1967, obtaining the following energy eigenvalue—modified for the spin by us:

$$W_S=m\omega_c+(n+\tfrac{1}{2})\omega_c'+(k+\tfrac{1}{2})\omega_z-(q+\tfrac{1}{2})\omega_m\ , \tag{4.3}$$

with $m=\pm\frac{1}{2}$, $n=0,1,2,3,\ldots$, $k=0,1,2,3,\ldots$, and $q=0,1,2,3,\ldots$, denoting spin, cyclotron, axial, and magnetron motion quantum numbers, respectively.

In this equation, ω_c' and ω_m are the classical (shifted) cyclotron frequency and the magnetron frequency described in Sec. III. The eigenfunction may be factorized

$$|\,mnkq\,\rangle=|\,m\,\rangle\,|\,nq\,\rangle\,|\,k\,\rangle\ . \tag{4.4}$$

For the state $|\,nq\,\rangle$ the expectation values of the squares of the cyclotron and magnetron orbit radii are

$$\begin{aligned}\langle\,nq\,|\,r_c^{\,2}\,|\,nq\,\rangle&=(2n+1)r_0^{\,2}\ ,\\ \langle\,nq\,|\,r_m^{\,2}\,|\,nq\,\rangle&=(2q+1)r_0^{\,2}\ ,\end{aligned} \tag{4.5}$$

where the quantity r_0 is defined by

$$r_0^{\,2}\equiv\lambda\!\!\!^{-}_c\lambda\!\!\!^{-}_C \tag{4.6}$$

with $\lambda\!\!\!^{-}_C=1/m_0$ and $\lambda\!\!\!^{-}_c=1/\omega_c$ as Compton and cyclotron wavelengths, respectively. The corresponding transition matrix element is then given by

$$|\,\langle\,n+1,q\,|\,x\,|\,n,q\,\rangle\,|^2\approx(n+1)r_0^{\,2}/2\ . \tag{4.7}$$

The Pauli magnetic-moment—magnetic-field interaction has been introduced in the usual fashion by adding a term $\omega_c\sigma_z/2$ to the Hamiltonian and the factor $|\,m\,\rangle$ to the wave function. Allowance has not yet been made for the anomalous magnetic moment.

B. Dirac equation

The most striking aspect of the relativistic spectrum of an electron with an anomalous magnetic moment moving only perpendicular to a homogeneous magnetic field $B_0\hat{\mathbf{z}}$ and *unconfined* in the axial direction is the exact independence of the anomaly frequency $\omega_a\equiv\tilde{\omega}_s-\tilde{\omega}_c$ (or spin-cyclotron beat frequency) on the excitation energy in the cyclotron motion W_c, while spin and cyclotron frequencies $\tilde{\omega}_s(W_c)$ and $\tilde{\omega}_c(W_c)$ of course show the familiar relativistic shift. This exact invariance of ω_a obviously calls for stringent experimental tests at cyclotron excitation energies of 1 MeV and more in the future. This invariance is clearly reflected in the relativistic energy eigenvalue (see Fig. 8)

$$E_D=(m_0^{\,2}+2jm_0\omega_c)^{1/2}+m\omega_a\ , \tag{4.8}$$

with

$$j\equiv m+n+\tfrac{1}{2}\ ,$$

obtained for the special case of vanishing axial confinement and energy, by an exact solution of the Dirac equation for zero electric field:[35]

$$(\boldsymbol{\alpha}\cdot\boldsymbol{\pi}+\rho_3m_0+\rho_3\omega_a\sigma_z/2)\psi=E_D\psi\ , \tag{4.9}$$

where $\boldsymbol{\alpha}$ and ρ_3 are Dirac matrices. Here m_0 is the rest mass and the term $\rho_3\omega_a\sigma_z/2$ takes the anomalous magnetic moment into account. A straight-forward derivation of Eq. (4.8) may be obtained by spelling out the four simultaneous differential equations equivalent to Eq. (4.9) and proceeding in a fashion similar to that used by Rabi[36] in

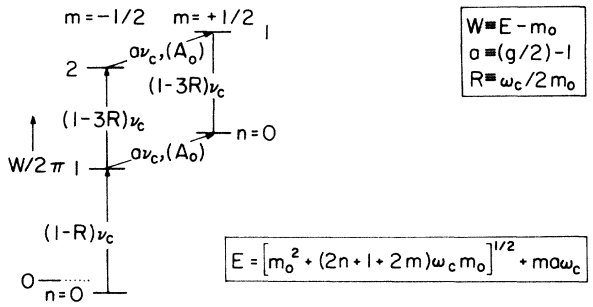

FIG. 8. Simplified energy level diagram for geonium (schematic). The five lowest relativistic energy eigenvalues are shown. Vanishing axial and magnetron frequencies and excitations are assumed.

1928. The result is a special case of the general exact eigenvalue expression for nonvanishing axial motion

$$E_D=\{[(m_0{}^2+2jm_0\omega_c)^{1/2}+m\omega_a]^2+\pi_z{}^2\}^{1/2} \quad (4.10)$$

derived by Ternov, Bagrow, and Zhudovski,[35] and by Tsai.[37] It is very useful to expand (4.10) retaining only terms up through (kinetic energy)$^2/m_0$:

$$\begin{aligned}W_D&\equiv E_D-m_0\\&=j\omega_c-j^2\omega_c{}^2/2m_0+\pi_z{}^2/2m_0-\pi_z{}^4/8m_0{}^3\\&\quad-j\omega_c\pi_z{}^2/2m_0{}^2+m\omega_a-m\omega_a\pi_z{}^2/2m_0{}^2\ .\end{aligned} \quad (4.11)$$

Here the first term gives the (ordinary) eigenvalues of cyclotron and Dirac spin motion energies while the second yields the relativistic shifts in ω_s, ω_c due to the kinetic energy in spin and cyclotron motion. The relativistic axial kinetic energy is expressed in the third and fourth terms. The sixth term is the anomalous magnetic moment contribution. The fifth and seventh terms are cross terms showing the relativistic decrease in spin, cyclotron, and anomaly frequencies with increasing kinetic energy in the axial motion.

C. Pauli approximation

An exact solution of the Dirac equation in the presence of both magnetic and electric fields is not possible. However, when suitably modified for our purposes, Pauli's two-component Hamiltonian[38] provides a very good approximation to the Dirac equation:

$$\begin{aligned}H_P&=\pi^2/2m_0+U+\omega_c\sigma_z/2-(W_S-U)^2/2m_0\\&\quad+(e/4m_0{}^2)\boldsymbol{\sigma}\cdot(\mathbf{E}\times\boldsymbol{\pi})\ ,\end{aligned} \quad (4.12)$$

where $\mathbf{E}$ is the electric field associated with electric potential $\phi(r,z)$ such that $U=-e\phi$ and eigenvalue $W_P\equiv E_P-m_0$. Recognizing the first three terms as the Schrödinger Hamiltonian H_S for a Dirac electron, we have

$$H_P=H_S+H_r\ , \quad (4.13)$$

where H_r is a small relativistic correction term. In the spin-orbit coupling term we have replaced the canonical momentum $\mathbf{p}$ with the kinetic term $\boldsymbol{\pi}$ to get agreement with the classical limit.

Treating H_r as a small perturbation, we obtain the eigenvalue W_P for H_P in the form

$$W_P=W_S+\langle mjkq\,|\,H_r\,|\,mjkq\rangle\ , \quad (4.14)$$

where $|\,mjkq\rangle$ is a Schrödinger eigenfunction. Even simpler and quite sufficient for our purposes is to neglect relativistic electric field effects completely and to approximate $\langle H_r\rangle$ by the expectation value of the appropriate terms of the B-field-only solution, Eq. (4.11)

$$\begin{aligned}\langle H_r\rangle&\approx-j^2\omega_c{}^2/2m_0-\langle\pi_z{}^4\rangle/8m_0{}^3-j\omega_c\langle\pi_z{}^2\rangle/2m_0{}^2\\&=-j^2\omega_c{}^2/2m_0-\tfrac{3}{16}(k+\tfrac{1}{2})^2\omega_z{}^2/m_0\\&\quad-\tfrac{1}{2}j\omega_c(k+\tfrac{1}{2})\omega_z/m_0\ .\end{aligned} \quad (4.15)$$

We obtain the final energy eigenvalue $\tilde{W}_P$ which includes the anomalous moment contribution W_a, by adding the expectation value of the appropriate terms in (4.11) to W_P:

$$\tilde{W}_P=W_P+W_a\ , \quad (4.16)$$

where

$$\begin{aligned}W_a&=m\omega_a-m\omega_a\langle\pi_z{}^2\rangle/2m_0{}^2\\&=m\omega_a-m\omega_a(k+\tfrac{1}{2})\omega_z/2m_0\ .\end{aligned} \quad (4.17)$$

In an alternate approach, we may add to H_P a term H_a taken from an expansion of Eq. (A15) of Mendlowitz and Case,[39]

$$H_a\approx\sigma_z\omega_a/2-\omega_a(\boldsymbol{\sigma}\cdot\boldsymbol{\pi})\pi_z/4m_0{}^2 \quad (4.18)$$

to obtain $\tilde{H}_P=H_P+H_a$. For the final Pauli Hamiltonian with anomalous magnetic moment contribution we may now write

$$\begin{aligned}\tilde{H}_P&=\pi^2/2m_0+U+\omega_c\sigma_z/2-(W_S-U)^2/2m_0\\&\quad+(e/4m_0{}^2)\boldsymbol{\sigma}\cdot(\mathbf{E}\times\boldsymbol{\pi})+(\omega_a/2)\sigma_z\\&\quad-\omega_a(\boldsymbol{\sigma}\cdot\boldsymbol{\pi})\pi_z/4m_0{}^2\ .\end{aligned} \quad (4.19)$$

More complete expressions obtained on the basis of Foldy-Wouthuysen transformations have been given in the past by Gräff, Klempt, and Werth[5] and by Brown.[40]

Taking the expectation value of H_a, we find that

$$\langle H_a\rangle=m\omega_a-m\omega_a(k+\tfrac{1}{2})\omega_z/2m_0 \quad (4.20)$$

in agreement with the term W_a used above in (4.17). The final expression for the energy eigenvalue is

$$\begin{aligned}\tilde{W}_P&=W_S+\langle H_r\rangle+\langle H_a\rangle\\&=j\omega_c-j^2\omega_c{}^2/2m_0+(k+\tfrac{1}{2})\omega_z-\tfrac{3}{16}(k+\tfrac{1}{2})^2\omega_z{}^2/m_0-j\omega_c(k+\tfrac{1}{2})\omega_z/2m_0+m\omega_a\\&\quad-m\omega_a(k+\tfrac{1}{2})\omega_z/2m_0-(q+\tfrac{1}{2})\omega_m\ .\end{aligned} \quad (4.21)$$

D. Transition frequencies

For the cyclotron transition $(jmkq)\rightarrow(j'mkq)$, $j'=j+1$, one has from Eq. (4.21)

$$\omega_{jj'}=\omega_c[1-(k+\tfrac{1}{2})\omega_z/2m_0-(j+\tfrac{1}{2})\omega_c/m_0]\ . \quad (4.22)$$

For $k=0$ and as $\omega_z\ll\omega_c$ this may be approximated by

$$\omega_{jj'}\approx\omega_c[1-(j+\tfrac{1}{2})\omega_c/m_0] \quad (4.23)$$

which puts into evidence the relativistic mass increase proportional to the kinetic energy in cyclotron and spin

motions. For $m=-\frac{1}{2}$, the quantum number $j=n+\frac{1}{2}+m$ $(n=0,1,2,3,\ldots)$ takes on the values $j=0,1,2,3,\ldots$, while for $m=+\frac{1}{2}$, only $j=1,2,3,\ldots$ are possible. Consequently, the cyclotron spectrum consisting of equally spaced components, separated by the additional term, $2R\omega_c \equiv \omega_c{}^2/m_0$, stretches to lower frequencies beginning at $\omega_c(1-R)$ for $m=-\frac{1}{2}$, but starting at $\omega_c(1-3R)$ for $m=+\frac{1}{2}$, see Fig. 9. Provided one manages to solve the problems of ultrahigh-resolution cyclotron-resonance spectroscopy, one gets the determination of the spin state for free.[26(d)]

The relativistic shift due to the kinetic energy in the axial motion takes the form

$$\Delta^z\omega_{jj'}/\omega_c = -W_z/2m_0 \ , \tag{4.24}$$

where W_z is the axial energy. The frequency of the most important spin-cyclotron difference frequency transition $(jmkq)\rightarrow(jm'kq)$, $m=-\frac{1}{2}$, $m'=+\frac{1}{2}$,

$$\omega_{mm'}=\omega_a[1-(k+\tfrac{1}{2})\omega_z/2m_0] \ , \tag{4.25}$$

shows only a relativistic shift due to the axial motion and of the same relative magnitude as the shift in $\omega_{jj'}$,

$$\Delta^z\omega_{mm'}/\omega_a = -W_z/2m_0 \ . \tag{4.26}$$

As a numerical example, if one has $W_z=\omega_c$, $\omega_c/2\pi=1.4\times10^{11}$ Hz, then, with $m_0/2\pi=1.2\times10^{20}$ Hz, the values $\omega_c{}^2/m_0=2\pi\times160$ Hz and $\Delta^z\omega_{jj'}/\omega_c=\Delta^z\omega_{mm'}/\omega_a=-5.8\times10^{-10}$ follow.

E. Anomaly resonance

We discuss this resonance only in the limit of vanishing excitation and first for vanishing electrical trapping fields (see Fig. 10). As the electron moves through the magnetic bottle field along a cyclotron orbit centered on the axis, it sees a magnetic field $-\beta z_a \mathbf{r}_c$ rotating at the cyclotron frequency with $\mathbf{r}_c$ taken in the xy-plane. (See Sec. V for complete description of the bottle field). By simultaneously exciting an axial oscillation at ω_a of amplitude z_a, this rotating field is also made to oscillate in amplitude:

$$\mathbf{b}_c = -\beta \mathbf{r}_c z_a \cos(\omega_a t) \ . \tag{4.27}$$

Decomposing the oscillating vector of amplitude $2b_a$ into two counter-rotating ones of magnitude

$$b_a = -\beta z_a r_c/2 \ , \tag{4.28}$$

one component in the laboratory frame will now rotate at $\omega_c+\omega_a$ and cause spin flips with a Rabi frequency

$$\omega_{\mathrm{Ra}}=\beta\mu_B z_a r_c/\hbar \ . \tag{4.29}$$

In a frame rotating with the $\mathbf{b}_a$ field, the expectation value of the spin vector initially in the $m=+\frac{1}{2}$ state will precess away from the z axis, making an angle $\theta=\omega_{\mathrm{Ra}}t$ with it after a time t. The corresponding growing fractional population f in the $m=-\frac{1}{2}$ level is related to θ:

$$f=\theta^2/4=\omega_{\mathrm{Ra}}{}^2t^2/4, \quad \theta\ll1 \ . \tag{4.30}$$

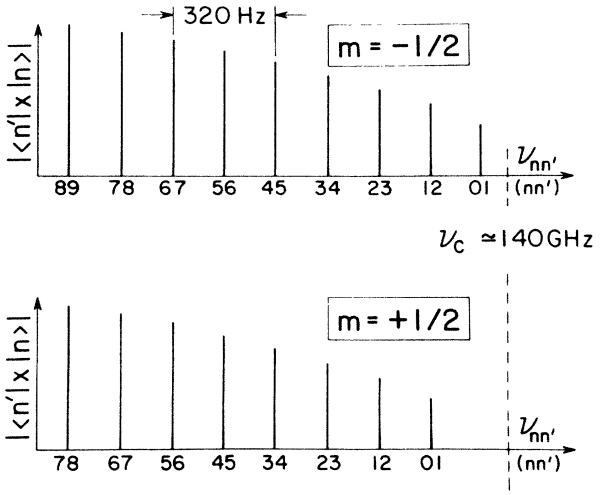

FIG. 9. Relativistic cyclotron spectra in geonium. For a field of ≈5 T, the value of the matrix element $x_{n'n}=\langle n'\,|\,x\,|\,n\rangle$ is plotted vs frequency for $n\rightarrow n'=n+1$ transitions between the lowest Rabi-Landau levels. Note spin-dependence of the spectrum.

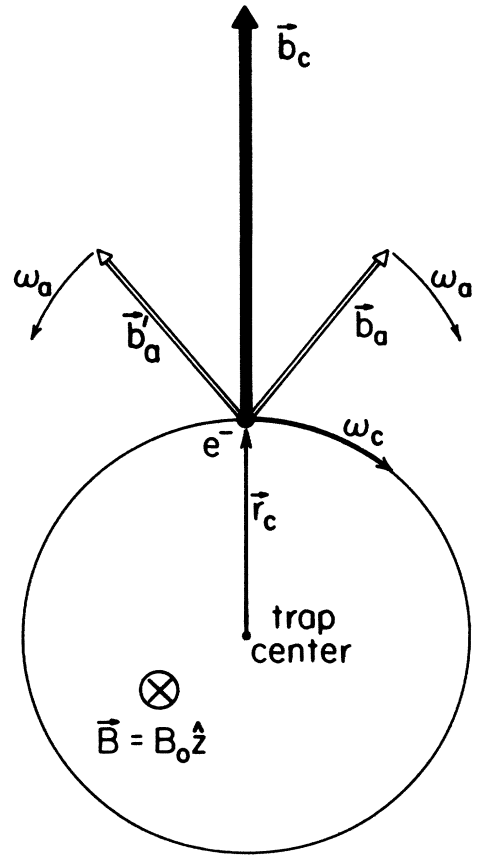

FIG. 10. Spin flips via assisted Majorana flops. All vectors shown lie in the plane of the drawing, which in turn is perpendicular to and rotates at ω_c around the z axis and lies at $z=z_a$ above the center of the magnetic bottle and the trap center. The forced oscillation of z at ω_a causes the component $\mathbf{b}_c$ of the bottle field seen by the electron to oscillate in amplitude. The oscillating $\mathbf{b}_c$ field is now decomposed into two components counter-rotating at $\pm\omega_a$. The "right" component $\mathbf{b}_a$ rotates at $\omega_c+\omega_a=\omega_s$ in the laboratory frame and causes the spin to flip.

We compare this with the quantum-mechanical rate for the transition $(mn)\rightarrow(m'n')$, $m=+\frac{1}{2}$, $m'=-\frac{1}{2}$, $n'=n+1$. Assuming at $t=0$ state amplitudes $a_{mn}(0)=1$, $a_{m'n'}(0)=0$, time-dependent perturbation theory gives

$$a_{m'n'}(t)=(-i/\hbar)\int_0^t H'_{m'n'mn}e^{-i\omega_a t'}dt' \tag{4.31}$$

with

$$H'=-\boldsymbol{\mu}\cdot\mathbf{b}_c\ . \tag{4.32}$$

Factorizing the matrix element yields

$$H'_{m'n'mn}=\tfrac{1}{2}\beta z_a(e^{i\omega_a t'}+e^{-i\omega_a t'})\times(\mu_{xm'm}x_{n'n}+\mu_{ym'm}y_{n'n})\ . \tag{4.33}$$

With[34] $\mu_{ym'm}=-i\mu_{xm'm}$ and $y_{n'n}=ix_{n'n}$, one finds for the population of the $m'n'$ level

$$f\equiv|a_{m'n'}(t)|^2=\omega_{\mathrm{Ra}}{}^2t^2/4 \tag{4.34}$$

with

$$\omega_{\mathrm{Ra}}=\beta\mu_B z_a 2x_{n'n}/\hbar\ . \tag{4.35}$$

For large n, both the cyclotron radius $r_0(2n+1)^{1/2}$ and $2x_{n'n}=r_0(2n+2)^{1/2}$ converge to the classical value r_c, yielding the equivalence of Eqs. (4.29) and (4.35).

The broadening of the anomaly resonance caused by the modulation of the magnetic field due to random, thermal *axial* motion through the auxiliary magnetic bottle is discussed in Secs. II and VI. Here, we are only interested in the natural width which remains, even if the axial motion is cooled to absolute zero. At zero axial temperature the classical, nonrelativistic cyclotron resonance ($n\gg1$) has only the natural width $\gamma_c=1/\tau_c$. Classically, one therefore expects the thermally excited cyclotron motion to have a spectrum of the same width γ_c. We denote the corresponding spectral range by $[\omega_c]$. For zero-width ω_a excitation (i.e., using a sharp drive frequency ω_{ad}), the rotation of the $\mathbf{b}_a$ field then has a spectral width γ_c likewise. By contrast, the pure spin flip $(mn)=(+\frac{1}{2}n)\leftrightarrow(-\frac{1}{2}n)$ has practically a zero width: ω_s is sharp. The spin-resonance condition, $\omega_s=[\omega_c]+\omega_{ad}$, may therefore be satisfied by a spread of ω_{ad} values of width $\gamma_a=\gamma_c$: the ω_a transition also has the width γ_c.

The quantum-mechanical analysis of the width of the ω_a resonance is complex. However for the most important transition $(mn)=(+\frac{1}{2}0)\leftrightarrow(-\frac{1}{2}1)$, which we now denote as the A_0 transition (see Fig. 8), we may argue that the natural width is again γ_c. This follows because the $(-\frac{1}{2}1)$ level has the finite lifetime τ_c due to spontaneous cyclotron transitions to the $(-\frac{1}{2}0)$ ground state.

We are now ready to discuss the rate at which the ω_a drive induces A_0 transitions. Again, we do this first only in the limit of vanishing drive and zero axial temperature. Denoting the population of the $(-\frac{1}{2}1)$ level by f, we may write its rate of change df/dt as the sum of two terms

$$df/dt=(df/dt)_d+(df/dt)_s \tag{4.36}$$

reflecting the contributions due to the drive and the spontaneous transitions to the ground state, respectively. With $(df/dt)_s=-f/\tau_c$, and using (4.34), Eq. (4.36) now takes the form

$$df/dt=\omega_{\mathrm{Ra}}f^{1/2}-f/\tau_c\ . \tag{4.37}$$

For a weak drive, $\gamma_a\gg\omega_{\mathrm{Ra}}$, and $f=0$ [i.e., a population of 1 in the $(+\frac{1}{2}0)$ level] at $t=0$, the population f will assume a small quasiequilibrium value f_e after the short time $2\tau_c$. By setting $df/dt=0$ in (4.37), one finds

$$f_e=\omega_{\mathrm{Ra}}{}^2\tau_c{}^2\ . \tag{4.38}$$

In equilibrium, the A_0-transition rate Γ_a for $(+\frac{1}{2}0)\rightarrow(-\frac{1}{2}1)$, at which the drive fills the $(-\frac{1}{2}1)$ level, must equal the rate at which the spontaneous transitions empty it:

$$f_e/\tau_c=\omega_{\mathrm{Ra}}{}^2\tau_c=\Gamma_a\ . \tag{4.39}$$

Because of various causes however, the experimentally observed width γ'_a of the anomaly resonance will be larger than $\gamma_a=1/\tau_c$ and the rate of induced transitions will be reduced to

$$\Gamma'_a=\Gamma_a\gamma_a/\gamma'_a=\omega_{\mathrm{Ra}}{}^2/\gamma'_a\ . \tag{4.40}$$

In the above analysis,

$$\tau_c=3m_0c^3/4e^2\omega_c{}^2\ , \tag{4.41}$$

which is the classical decay time, and using (4.35),

$$\omega_{\mathrm{Ra}}=\sqrt{2}\,\beta\mu_B z_a r_0/\hbar \tag{4.42}$$

applies.

Finally, the assumption that the cyclotron orbit be centered on the trap axis is not essential. Shifting the origin and instantaneous guiding center of the cyclotron motion according to $x=\xi+a$, $y=\eta+b$, and $z=\zeta$ yields for the auxiliary magnetic bottle field

$$\begin{aligned} b_\xi&=-\beta(\zeta\xi+\zeta a)\ ,\\ b_\eta&=-\beta(\zeta\eta+\zeta b)\ ,\\ b_\zeta&=\beta[\zeta^2-\tfrac{1}{2}(\xi+a)^2-\tfrac{1}{2}(\eta+b)^2]\ . \end{aligned} \tag{4.43}$$

At $(\xi,\eta,\zeta)=(0,0,0)$, the electron still sees the same rotating $\mathbf{b}_a$ field. The field components $\beta\zeta a$ and $\beta\zeta b$ have no spectral components at ω_s and are averaged to zero by the axial motion. The static component reduces the B_0 field by $\beta(a^2+b^2)/2$. Therefore, switching on the electric trapping field (thus producing a moving guiding center via the magnetron motion) leaves the above discussion essentially unaffected.

V. CONTINUOUS STERN-GERLACH EFFECT

We detect the ω'_a, ω'_c, and ω_m transitions in geonium, all of which are associated with a change in the z component of the total magnetic moment μ_z, by the "continuous" Stern-Gerlach effect[41] which is more fully discussed in a separate paper.[14] Here we need only note that to realize this effect, an auxiliary weak magnetic bottle is superimposed onto the electric trapping potential and serves to make the axial oscillation frequency slightly dependent on μ_z. This weak auxiliary magnetic bottle—produced by a

nickel wire (with technical details to be discussed in a later paper)—causes the magnetic field to deviate from the uniform value $B_0=B_z$ by

$$b_x=-\beta zx\ ,$$
$$b_y=-\beta zy\ , \tag{5.1}$$
$$b_z=\beta(z^2-r^2/2)\ ,$$

where $r^2=x^2+y^2$ and $\beta\approx 150$ G/cm^2 for the present bottle. The magnetic pseudopotential $U_m=-\mu_z(B_0+b_z)$ must be evaluated in an eigenstate of the μ_z operator. The corresponding eigenvalues of this magnetic moment operator are

$$\mu_z^{mnq}=-2[j+am+(\omega_m/\omega_c)q]\mu_B\ . \tag{5.2}$$

Here, a is the anomalous-magnetic-moment contribution, $j=m+n+\frac{1}{2}$, and m, n, k, and q are spin, cyclotron, axial, and magnetron motion quantum numbers, respectively. Therefore, the z-dependent part $U_m'=-\mu_z b_z$ has the value

$$\langle U_m'\rangle=2[j+(\omega_m/\omega_c)q]\mu_B\beta(z^2-r^2/2)\ , \tag{5.3}$$

dropping the insignificant term am. When combined with the usual electric potential associated with the harmonic axial oscillation, one finds that $\omega_z\approx 2\pi\times 60$ MHz is perturbed (i.e., shifted) by this magnetic coupling [see Eqs. (2.3) and (2.8)] according to

$$\delta\omega_z/\omega_z=2[j+(\omega_m/\omega_c)q]\beta Z_0{}^2\mu_B/eU_0\ . \tag{5.4}$$

This relation may be rewritten using

$$\delta\equiv(D_z^m/D_z^e)\omega_z\ , \tag{5.5}$$

where D_z^e is the depth of the usual electric well

$$D_z^e\mp eU_0/2\approx 5\text{ eV} \tag{5.6}$$

and D_z^m is the depth of the magnetic bottle well between the cap electrodes separated by $2Z_0$ as seen by a magnetic moment $-\mu_B$:

$$D_z^m=\beta Z_0{}^2\mu_B\approx 0.12\ \mu\text{eV}\ . \tag{5.7}$$

Thus, Eq. (5.4) can be written as

$$\delta\omega_z=[j+(\omega_m/\omega_c)q]\delta\ . \tag{5.8}$$

The discrete shift $\delta\omega_z$ is primarily a function of the slowly varying spin quantum number m and the quickly varying cyclotron quantum number n. In our mode of operation, the magnetron quantum number is usually reduced to such a small value that its contribution to $\delta\omega_z$ may be neglected. The apparatus responds fast enough, that both spin and cyclotron states are reduced to μ_z eigenstates identical to the energy eigenstates which are characterized by m and n. As one application of Eq. (5.8), the corresponding frequency shift associated with a spin flip simply becomes δ:

$$\omega_z(\uparrow)-\omega_z(\downarrow)=\delta\approx 2\pi\times(1.3\pm 0.2)\text{ Hz}\ . \tag{5.9}$$

As is evident from this analysis, the determination of the spin state must take the form of a resonance frequency measurement.

Another result of perturbing the magnetic field in this fashion [see Eq. (5.1)] is the dependence of the average magnetic field upon the axial quantum state. For an electron oscillating in the axial direction along the axis of symmetry,

$$\delta B\equiv B(z)-B_0=\beta z^2\ . \tag{5.10}$$

Since the axial energy W_z averaged over a period has the form

$$\langle W_z\rangle=m_0\omega_z{}^2\langle z^2\rangle \tag{5.11a}$$

and

$$\langle W_z\rangle=k\hbar\omega_z\quad(k\gg 1)\ , \tag{5.11b}$$

the change in the *effective* average magnetic field becomes

$$\langle\delta B\rangle=\beta k\hbar/m_0\omega_z\ . \tag{5.12}$$

Using (2.3), (3.2), and (5.5), the field dependence takes the form

$$\frac{\langle\delta B\rangle}{B_0}=k\left[\frac{\delta}{\omega_c}\right]\ . \tag{5.13}$$

As a consequence, both the cyclotron and the spin-precession frequencies have the form

$$\omega_c=\omega_{c0}+k\delta,\quad \omega_s=\omega_{s0}+k\delta\ , \tag{5.14}$$

where the dependence on the instantaneous axial quantum number is due to the perturbing magnetic bottle.

VI. LINE SHAPE

As already mentioned in Sec. II the line shape in the current geonium experiments is dominated by the modulation of the B field caused by the thermal random amplitude fluctuations of the ω_z motion in the inhomogeneous field of the magnetic bottle. The characteristic time of these fluctuations is similar to τ_z, the damping time of the ω_z motion due to coupling with the LC detection circuit. Now it is relatively easy to lengthen τ_z by detuning ω_z away from the LC circuit resonance but very difficult[42] to shorten it below the value optimal for detection. This eliminates the tempting possibility of averaging out the bottle induced linewidth by making the fluctuations very fast. The opposite alternative of making the time τ_z much longer than the inverse width of the modulation range (as given on a frequency scale) and thereby realizing a simple quasistationary line shape is already well approximated in the current geonium experiments for the cyclo tron resonance in the limit of vanishing ω_z detection drive, see Fig. 11. It should be possible to increase τ_z to ≈ 1 s in order to obtain the same simple vertical-rise—exponential-decay line shape for the ≈ 6 Hz wide ω_a' resonance, see Fig. 12, as is observed for the cyclotron resonance. How may this line shape be analyzed[26(d)] at the present time? In the limit of very slow relaxation of the ω_z motion, and very small ω_c'-resonance intrinsic linewidths, the shape for the ω_c'-resonance signal S_c should be given by

$$S_c(\omega)\begin{cases}=0 & \text{for } \omega\le\omega_{c0}'\ ,\\ \propto\exp(\omega_{c0}'-\omega/\Delta\omega_c) & \text{for } \omega>\omega_{c0}'\ .\end{cases} \tag{6.1}$$

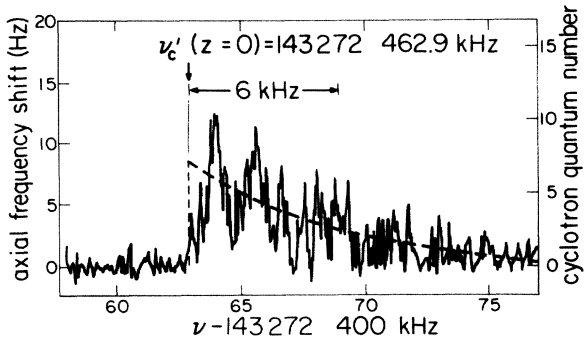

FIG. 11. Geonium cyclotron resonance. The vertical rise-exponential decay line shape exhibiting a signal strength decline to $1/e$ for a 6-kHz displacement reflects the proportionality of the average magnetic bottle field seen by the electron to the instantaneous thermally excited axial energy. At an axial temperature of 16 K the nearly vertical edge allows determination of ν_c' when the electron is at the bottom of the magnetic well ($z=0$) to ~ 500 Hz.

Here, $\Delta\omega_c \equiv (e\beta k_B/m_0{}^2 c\omega_z{}^2)T_z$ denotes the frequency deviation parameter and can be shown using Eq. (5.5) to equal $(k_B T_z/\hbar\omega_z)\delta$. For example, the resonance is excited at $\omega=\omega_c'(W_z)>\omega_{c0}'$ with the relative probability

$$P=\exp(-W_z/k_B T_z) \tag{6.2}$$

for the occurrence of the instantaneous axial energy W_z. Since it follows that

$$\omega_c'(W_z)-\omega_{c0}' \propto \langle b_z\rangle_{\rm av} \propto \langle z^2\rangle_{\rm av} \propto W_z\ , \tag{6.3}$$

we may write

$$P=\exp(\omega_{c0}'-\omega/\Delta\omega_c)\ , \tag{6.4}$$

and for our values, $T_z \approx 2.70\Delta\nu_c$ (K/kHz). Inspection of Fig. 11 shows a width $\Delta\nu_c \approx 6$ kHz and $T_z \approx 16$ K for the axial temperature which is still appreciably higher than

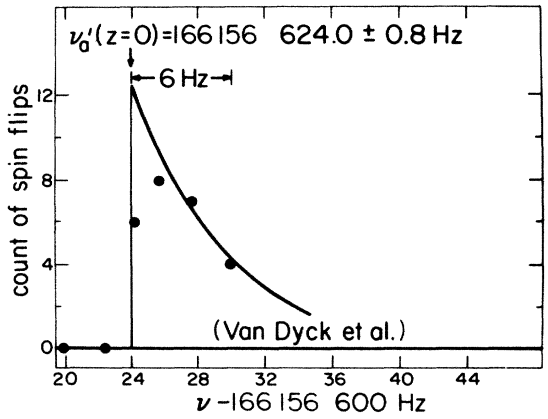

FIG. 12. Geonium anomaly resonance. The line shape is similar to that of Fig. 11 and the characteristic ~ 6 Hz displacement is also that expected for $T_z \approx 16$ K. For each data point, spin flips occurring in 24 interaction-measurement periods were counted.

the 4-K liquid-helium boiling point. The important feature is the abrupt rise in signal for $\omega=\omega_{c0}'$ which is associated with the excitation occurring when the electron is at the bottom of the magnetic bottle in the center of the trap. The idealized conditions assumed are rather well approximated for the cyclotron resonance, and the $z=0$ edge of the resonance at $\approx 1.43\times 10^{11}$ Hz may now be determined to ≈ 500 Hz, i.e., 3 parts in 10^9 in a single measurement. The anomaly resonance data with a width $\Delta\nu_a \approx 6$ Hz may also be fitted to an exponential line shape, see Fig. 12. However, currently, the procedure is not well justified as the axial relaxation time τ_z was not long compared to $1/\Delta\nu_a$. Nevertheless, it may be reasonable to determine the line "edge" of the 1.66×10^8 Hz resonance to a small fraction of the frequency deviation $\Delta\nu_a \equiv \Delta\nu_c(\nu_a'/\nu_c')$, namely, to ≈ 0.8 Hz or 5 parts in 10^9.

Specifically the above preconditions for obtaining the simple vertical-edge–exponential-decline line shape may be fulfilled by *pulsed* ω_c', ω_a' excitation and detection. Excitation and detection intervals should be no longer than cyclotron and spin relaxation times, respectively, namely, at $B_0 \approx 5$ T excitation intervals of 0.1 s and say, 20 s, but long compared to $\tau_z \geq 50$ ms. Also $\tau_z \gg 1/\Delta\nu_c$ and $\tau_z \gg 1/\Delta\nu_a$ must hold. For the ω_a' resonance this calls for different τ_z values, namely, $\tau_z \approx 1$ s during the ω_a'-excitation interval, and $\tau_z = 50$ ms during the subsequent ω_z-measurement interval.

Lastly, it remains to look into any contributions by the combined auxiliary axial ω_a' drive and the thermal amplitude z_B to the magnetic-bottle broadening. The total (complex) axial oscillation coordinate is given by

$$\tilde{z}=z_B\exp[i(\omega_z t+\phi)]+z_a\exp(i\omega_a' t) \tag{6.5}$$

with z_B and ϕ varying slowly with characteristic time $2\tau_z$ (thus reflecting Brownian motion) with both z_B, z_a real. From

$$\tilde{z}=\exp[i(\omega_z t+\phi)]\{z_B+z_a\exp[i(\omega_a'-\omega_z)t-i\phi]\}\ , \tag{6.6}$$

it follows that

$$|\tilde{z}|^2=z_B{}^2+z_a{}^2+2z_B z_a\cos[(\omega_a'-\omega_z)t-\phi]\ . \tag{6.7}$$

Since for our experiments, $\omega_a'-\omega_z \gg \Delta\omega_a$ or $\Delta\omega_c$ and $z_B > z_a$, we find that the cross term contributes only distant, very weak spectral components to the ω_c', ω_a' resonances. However, the constant $z_a{}^2$ term does produce a small positive shift of the $z=0$ edges toward higher frequencies. Identical effective magnetic fields for anomaly and cyclotron resonances may be guaranteed by leaving the ω_a' excitation on also when the ω_c' resonance is being recorded. Numerical estimates of this magnetic field shift give <10 ppb for the current experiments, a negligible value.

VII. SUMMARY

By solving the old problem of performing a Stern-Gerlach type of experiment on a free electron, we have measured the electron's g factor with unrivaled precision by an rf resonance technique. However, the introduction

of the inhomogeneous Stern-Gerlach field (or bottle field) exerts a price, when carrying out spin and cyclotron resonance experiments. Thus, much of the experimental effort is devoted to overcoming undesirable side effects of the inhomogeneous field. As our technique works for, and in fact requires, a quasipermanently confined individual electron, we avoid the intractable space-charge shifts limiting earlier efforts, in which clouds of electrons were studied.

As an important part of our experiment, we had to attempt a solution of one of the most basic problems in physics: namely, the localization of a single atomic particle in laboratory space.[4(a)] We have made considerable progress here, both by conventional cooling of the trapped electron via immersion of the trap in liquid helium, and by developing a novel radio-frequency sideband cooling technique. In fact, we appear to hold the record for quasipermanent close localization of an atomic particle in vacuum, which has given a few otherwise faceless electrons and positrons an identity lasting up to several months.

Localization and cooling make the small change in the magnetism of the electron associated with a spin flip now detectable, and minimize broadening of the resonance lines associated with the Brownian motion in the inhomogeneous bottle field. For ease of detection, this inhomogeneous field cannot be reduced below a minimum value and therefore remains the principal cause of line broadening, which limits the precision of the g-factor measurement. Nevertheless, by measuring the difference $\omega_s - \omega_c$ of the spin and cyclotron frequencies directly instead of ω_s, and by separating transition and detection cycles in time, it has been possible to reduce the width of the critical $\omega_s - \omega_c$ transition to a small multiple of the natural value of ≈ 1 Hz.

A rudimentary analysis of the Brownian-motion-induced line shape has been performed.[43] The relativistic quantum mechanics of geonium has been discussed and it has been shown that relativistic shifts are easily controlled in the experiments. It has been estimated that the relativistic fine structure should be detectable and may form the basis of an alternate technique for the detection of spin flips, free of the drawbacks of an inhomogeneous magnetic field. Further details on the experiment will be reported in a sequel to this paper, and a more detailed paper describing the continuous Stern-Gerlach effect has appeared elsewhere.[14]

ACKNOWLEDGMENTS

We enjoyed conversations with many of our colleagues, especially D. Boulware, L. S. Brown, E. N. Fortson, G. Gabrielse, G. Janik, H. Lubatti, R. Peierls, L. Wilets, and R. W. Williams. One of us (H.G.D.) had extensive discussions with W. E. Lamb, Jr., E. M. Purcell, and I. I. Rabi. C. Cohen-Tannoudji, College de France, and L. S. Brown and G. Gabrielse also were kind enough to read the manuscript, to offer suggestions, and, after its submission, make available to us copies of related papers of their own prior to publication. The work was supported by the National Science Foundation under the "Single Elementary Particle at Rest in Free Space" project.

[1]R. H. Dicke, NASA Conference Report No. 2265, 1982, p. 646 (unpublished); H. A. Tolhoek, Rev. Mod. Phys. **28**, 277 (1956).

[2]W. H. Louisell, R. W. Pidd, and H. R. Crane, Phys. Rev. **91**, 475 (1953); **94**, 7 (1954).

[3]H. G. Dehmelt, Science **124**, 1039 (1956); Phys. Rev. **109**, 381 (1958).

[4](a) H. Dehmelt, in *Advances in Atomic and Molecular Physics,* edited by D. R. Bates and I. Estermann (Academic, New York, 1967), Vol. 3, p. 53; in *Advances in Atomic and Molecular Physics,* edited by D. R. Bates and I. Estermann (Academic, New York 1969), Vol. 5, p. 109; (b) in *Physics of Electronic and Atomic Collisions,* edited by J. S. Risley and R. Geballe (University of Washington Press, 1976), p. 857; (c) H. G. Dehmelt and F. L. Walls, Phys. Rev. Lett. **21**, **127** (1968); (d) H. G. Dehmelt and F. G. Major, *ibid.* **8**, 213 (1962).

[5]G. Gräff, F. G. Major, R. W. Roeder, and G. Werth, Phys. Rev. Lett. **21**, 340 (1968); G. Gräff, E. Klempt, and G. Werth, Z. Phys. **222**, 201 (1969).

[6]H. R. Crane, in *High Energy Physics with Polarized Beams and Targets,* edited by M. L. Marshak (AIP Conference Proceedings No. 35) (AIP, New York, 1976), p. 306; A. Rich, and J. C. Wesley, Rev. Mod. Phys. **44**, 250 (1972); R. Conti, D. Newman, A. Rich, and E. Sweetman, in *Precision Measurement and Fundamental Constants II,* edited by B. N. Taylor and W. D. Phillips (Natl. Bur. Stand., U. S. Spec. Publ. 617) (NBS, Washington, D.C., 1984), p. 207.

[7]L. Brillouin, C. R. Acad. Sci. Paris **184**, 82 (1927); Proc. Natl. Acad. Sci. U.S.A. **14**, 756 (1928). Brillouin proposed to stop a beam of slow electrons in a spin-dependent fashion by shooting it along the field axis into a magnetic field steeply rising to 3 T. Thereby, *one* spin direction is prevented from reaching an electron "counter." The later proposal by F. Bloch [Physica **19**, 821 (1953)] also uses a field with a strong gradient. This gradient is now pulsed and used to squeeze out of an electric well of depth $< 10^{-5}$ V and of unspecified shape all but those electrons in the nonmagnetic lowest Rabi-Landau level. Afterward, the gradient is turned off and spin or cyclotron resonance transitions depopulate the nonmagnetic ground state. Electrons, which have made such a transition, are forced out of the well and counted when the gradient is switched on again. For a detailed discussion of these and other proposals, see the reviews cited at the end of Sec. I.

[8]J. Mehra and H. Rechenberg, *The Historic Development of Quantum Theory* (Springer, New York, 1982), Vol. 1, Pt. 2, p. 696; W. Pauli, in *Exclusion Principle in Quantum Mechanics, Prix Nobel* in *Collected Scientific Papers,* edited by R. Kronig and V. F. Weisskopf (Interscience-Wiley, New York, 1964), Vol. 2, p. 1082/83.

[9]B. L. van der Waerden, in *Theoretical Physics in the Twentieth Century: A Memorial Volume for Wolfgang Pauli,* edited by M. Fierz and V. F. Weisskopf (Interscience, New York, 1960), pp. 199–244.

[10]P. A. M. Dirac, *The Principles of Quantum Mechanics,* 4th ed. (Clarendon, Oxford, 1958), p. 262.

[11]E. Schrödinger, Sitzungsb. Preuss, Akad. Wiss. Phys. Math.

Kl. **24**, 418 (1930); **3**, 1 (1932).
[12]K. Huang, Am. J. Phys. **20**, 479 (1952).
[13]W. Pauli, in *Le Magnetism, 6eme Conseil de Physique Solvay, Bruxelles 1930* (Gauthier-Villars, Paris, 1932), p. 217, reprinted in *Collected Scientific Papers* (Ref. 8), Vol. 2, p. 544, discussion by Bohr, Darwin, Dirac, Einstein, Fermi, Kapitza, Kramers, Richardson, and Van Vleck on p. 602; Jagdish Mehra, *The Solvay Conferences on Physics* (Reidel, Dordrecht, Boston, 1975), pp. 184 and 198.
[14]H. Dehmelt and P. Ekstrom, Bull. Am. Phys. Soc. **18**, 727, (1973); H. Dehmelt, Proc. Natl. Acad. Sci. U.S.A. **83**, 2291 (1986).
[15]J. H. Field, E. Picasso, and F. Combley, Usp. Fiz. Nauk **127**, 553 (1979) [Sov. Phys. Usp. **22**, 199 (1979)].
[16]T. Kinoshita and J. Sapirstein, in *Atomic Physics 9,* edited by R. S. Van Dyck, Jr. and E. N. Fortson (World Scientific, Singapore, 1984), p. 38.
[17]J. W. Cronin (private communication).
[18]P. S. Farago, in *Advances in Electronics and Electron Physics,* edited by L. Marton (Academic, New York, 1965), Vol. 21, p. 1.
[19]E. Klempt, Habilitations-Schrift, Universität Mainz, 1975.
[20]H. Dehmelt, in *Atomic Masses and Fundamental Constants,* edited by J. H. Sandars and A. H. Wapstra (Plenum, New York, 1976), Vol. 5, p. 499.
[21]H. A. Schuessler, in *Progress in Atomic Spectroscopy,* Part B, edited by W. Hanle and H. Kleinpoppen (Plenum, New York, 1979), p. 999.
[22]G. Werth, in *Progress in Atomic Spectroscopy,* Part C, edited by H. J. Beyer and H. Kleinpoppen (Plenum, New York, 1984), p. 151.
[23]D. J. Wineland, in *Precision Measurement and Fundamental Constants II* (Ref. 6), p. 83.
[24]D. J. Wineland, Wayne M. Itano, and R. S. Van Dyck, Jr., in *Advances in Atomic and Molecular Physics,* edited by B. Bederson and D. Bates (Academic New York, 1983), Vol. 19, p. 135.
[25]H. Dehmelt, Bull. Magn. Reson. **4**, 17 (1982); in *Advances in Laser Spectroscopy,* NATO ASI Series, Series B: Physics, Vol. 95, edited by F. T. Arecchi, F. Strumia, and H. Walther (Plenum, New York, 1983), p. 153.
[26](a) R. Van Dyck, Jr., P. Ekstrom, and H. Dehmelt, Nature (London) **262**, 776 (1976); (b) R. S. Van Dyck, Jr., P. B. Schwinberg, and H. G. Dehmelt, Phys. Rev. Lett. **38**, 310 (1977); (c) R. S. Van Dyck, Jr., P. Schwinberg, and H. Dehmelt, in *New Frontiers in High-Energy Physics,* edited by B. Kursunoglu, A. Perlmutter, and L. Scott (Plenum, New York, 1978), p. 159; (d) H. Dehmelt, in *Atomic Physics 7,* edited by Daniel Kleppner and Francis Pipkin (Plenum, New York, 1981), p. 337; (e) P. B. Schwinberg, R. S. Van Dyck, Jr., and H. G. Dehmelt, Phys. Lett. **81A**, 119 (1981).
[27]G. P. Lepage, in *Atomic Physics 7* (Ref. 26), p. 297.
[28]T. Kinoshita and W. B. Lindquist, Phys. Rev. Lett. **47**, 1573 (1981); Phys. Rev. D **27**, 853 (1983); **27**, 867 (1983); **27**, 877 (1983); **27**, 886 (1983).
[29]D. J. Wineland and H. G. Dehmelt, J. Appl. Phys. **46**, 919 (1975).
[30]D. Wineland, P. Ekstrom, and H. Dehmelt, Phys. Rev. Lett. **31**, 1279 (1973).
[31]R. S. Van Dyck, Jr., D. J. Wineland, P. A. Ekstrom, and H. G. Dehmelt, Appl. Phys. Lett. **28**, 446 (1976).
[32]S. Liebes, Jr. and P. Franken, Phys. Rev. **116**, 633 (1959).
[33]L. S. Brown and G. Gabrielse, Phys. Rev. A **25**, 2423 (1982).
[34]A. A. Sokolov and Y. G. Pavlenko, Opt. Spectrosc. (USSR) **22**, 1 (1967).
[35]I. M. Ternov, V. G. Bagrov, and V. C. Zhukovskii, Moscow Univ. Phys. Bull. **21**, 21 (1966).
[36]I. I. Rabi, Z. Phys. **49**, 507 (1928).
[37]W. Tsai, Phys. Rev. D **7**, 1945 (1973).
[38]See Eq. (12.11) of H. A. Bethe and E. E. Salpeter, in *Encyclopedia of Physics XXXV,* edited by S. Flügge (Springer, Berlin, 1957), p. 142.
[39]H. Mendlowitz and K. M. Case, Phys. Rev. **97**, 33 (1955).
[40]L. S. Brown (unpublished).
[41]W. Gerlach and O. Stern, Ann. Phys. (Leipzig) **74**, 673 (1924).
[42]Actually, by using a tiny superconducting coil for L, it may be possible to greatly reduce τ_z.
[43]A more refined analysis of the line shape has since been published: L. S. Brown, Ann. Phys. (N. Y.) **159**, 62 (1984).

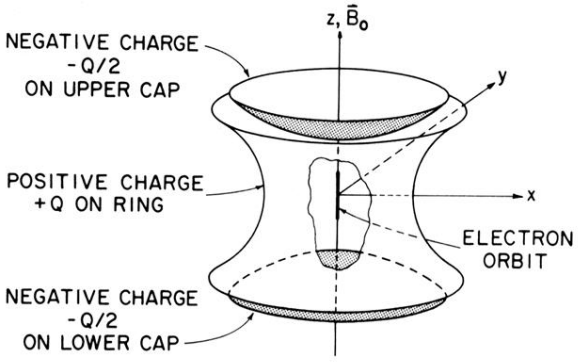

FIG. 1. *Monoelectron oscillator* mode of electron in Penning trap, the geonium "atom." The electron moves only parallel to the magnetic field $\mathbf{B}_0$ and along the symmetric axis of the electrode structure. Each time it gets too close to one of the negatively charged caps, it is turned around and an oscillatory motion results.